

When to Think and When to Look: Uncertainty-Guided Lookback

Jing Bi¹ Filippos Bellos² Junjia Guo³ Yayuan Li² Chao Huang¹ Yunlong (Yolo) Tang¹
Luchuan Song¹ Susan Liang¹ Zhongfei (Mark) Zhang³ Jason J. Corso² Chenliang Xu¹

¹University of Rochester ²University of Michigan ³Binghamton University

{jing.bi, yunlong.tang, chenliang.xu}@rochester.edu, {fbellos, yayuanli, jjcorso}@umich.edu
{jguo22, zzhang}@binghamton.edu, {chuang65, sliang22, lsong11}@cs.rochester.edu

Abstract

Test-time “thinking” (i.e., generating explicit intermediate reasoning chains) is known to boost performance in large language models and has recently shown strong gains for large vision–language models (LVLMs). However, despite these promising results, there is still no systematic analysis of how thinking actually affects visual reasoning. We provide the first such analysis with a large-scale, controlled comparison of thinking for LVLMs, evaluating 10 variants from the InternVL3.5 and Qwen3-VL families on MMMU_{val} under generous token budgets and multi-pass decoding. We show that more thinking is not always better: long chains often yield long-wrong trajectories that ignore the image and underperform the same models run in standard instruct mode. A deeper analysis reveals that certain short “lookback” phrases, which explicitly refer back to the image, are strongly enriched in successful trajectories and correlate with better visual grounding. Building on this insight, we propose uncertainty-guided lookback, a training-free decoding strategy that combines an uncertainty signal with adaptive lookback prompts and breadth search. Our method improves overall MMMU performance, delivers the largest gains in categories where standard thinking is weak, and outperforms several strong decoding baselines, setting a new state of the art under fixed model families and token budgets. We further show that this decoding strategy generalizes, yielding consistent improvements on five additional benchmarks, including two broad multimodal suites and math-focused visual reasoning datasets.

1. Introduction

Large vision language models (LVLMs) are rapidly becoming general-purpose visual assistants, expected to read charts, solve exam-style questions, and reason about diagrams at a level approaching human experts. At the same time, evaluation suites such as LMMs-Eval [53] highlight

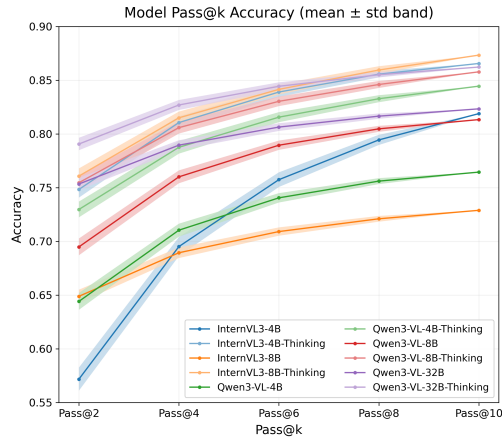


Figure 1. Pass@k accuracy on MMMU_{val} for 10 LVLM variants from the InternVL3.5 and Qwen3-VL families. Increasing the number of samples k (breadth) yields steep early gains for all models, especially smaller ones, while enabling the built-in thinking mode consistently shifts curves upward but with diminishing returns beyond Pass@8. This illustrates that additional sampling can often substitute for deeper test-time thinking and that the benefits of thinking depend strongly on model capacity.

that, despite impressive headline results, current LVLMs remain brittle across domains and task formats, motivating more principled ways of allocating test-time compute.

On the language side, *Thinking*—test-time chain-of-thought decoding, self-consistency, and reflection-style prompting—has emerged as a key ingredient for complex reasoning [14, 37, 50], delivering strong gains on text-only benchmarks. However, extending these techniques to multimodal settings is more delicate.

Recent studies show that LVLMs inherit the failure modes of language models while adding new cross-modal issues, such as over-reliance on text priors and visual hallucination [45, 57] with only a few families (e.g., Qwen2.5-VL and InternVL3) exhibit noticeably stronger visual grounding as capacity grows [55]. To better couple reasoning with perception, work on *visual CoT* has begun

to explicitly incorporate visual intermediates. Methods such as VCoT [30], Visual Sketchpad [17], and MathCanvas [33] endow models with drawing or diagram-editing capabilities that act as scratchpads for geometry and spatial reasoning, thus typically relying on extra supervision or tooling.

Meanwhile, LVLM families such as Qwen-VL and its successors [3, 4, 40] and InternVL3/3.5 [43, 59] expose explicit “thinking” modes. These models pair high-capacity language backbones with competitive visual front-ends and report state-of-the-art results on MMMU and related benchmarks. However, this trend raises three intertwined questions that are still poorly understood:

When does test-time thinking help visual reasoning?

Thinking is widely assumed to be beneficial, but we lack systematic study between instruct and thinking modes across model sizes, sampling budgets, and task categories.

How should we trade off breadth vs. depth of thinking?

We do not yet know how to best allocate test-time compute between sampling more reasoning paths (breadth) and using stronger reasoning modes (depth) in perception tasks.

Can we control thinking for better perception tasks?

Text-only CoT work on early exit and confidence (DEER [47], DeepConf [16], REFRAIN [34]) shows that blindly elongating chains can be wasteful or harmful, motivating LVLM decoding that reacts to visual grounding and uncertainty rather than token counts alone.

This paper addresses these questions through a systematic study of visual thinking in the latest InternVL3.5 [43] and Qwen3-VL [4] models. We focus on these two families because Qwen3 LLMs consistently outperform LLaMA-based counterparts, and both Qwen3-VL and InternVL3.5 are open-source state-of-the-art LVLMs with a large margin over other models; prior work [45, 57] also indicates that only these families exhibit strong visual reasoning.

Through controlled experiments and fine-grained analysis, we show that test-time thinking has a highly structured, non-uniform impact: its benefits depend strongly on model capacity, sampling budget, and task category. In particular, we find clear regimes where thinking helps and others where concise instruct decoding is preferable. Building on these observations, we propose *uncertainty-guided lookback*, a training-free decoding strategy. Instead of always “thinking more,” we monitor when the model’s ongoing chain is likely drifting and selectively trigger short, visually anchoring lookback prompts that refocus the reasoning on the image. This mechanism, optionally combined with a lightweight parallel exploration of more visually grounded continuations, turns our analysis of long-wrong vs. quiet-wrong behavior into a practical recipe for routing deliberation to the instances where visual thinking actually improve.

Overall, this work makes the following contributions:

A systematic analysis of visual thinking in LVLMs. We provide a large-scale study of thinking vs. instruct compar-

isons for latest models, disentangling breadth vs. depth of thinking and characterizing their effects across model sizes, categories, and difficulty levels.

A capacity-regularized token economy for visual reasoning. We show how language capacity and task difficulty jointly shape the cost and utility of thinking, exposing compute-equivalence trade-offs and highlighting when long-wrong” versus quiet-wrong” failures dominate.

Uncertainty-guided lookback for adaptive visual CoT. We introduce a training-free, model-agnostic decoding strategy. Across MMMU and five additional benchmarks, this method consistently improves accuracy over standard thinking while keeping or lowering the fraction of thinking tokens, with especially large gains in categories where naive thinking previously underperformed.

2. Related Work

2.1. Reasoning in LLMs

CoT prompting often boosts success on complex tasks, yet recent work details important limitations: benchmarking across modalities shows that reflection and test-time scaling help but can also cause overthinking on perception-heavy problems [5, 20]; generated rationales need not be faithful to internal computation [11]; CoT can obscure hallucination cues [12]; and gains may evaporate under distribution shifts [56]. These emerging limitations motivate our investigation into how thinking influence visual reasoning performance.

2.2. Visual Reasoning

Visual reasoning benchmarks increasingly minimize language priors to isolate perception–reasoning interplay. VERIFY emphasizes explanation fidelity and reports persistent gaps on abstract visual reasoning [6, 35]. Surveys and position papers underscore why *reasoning* (not just recognition) is central in multimodal settings and outline evaluation pitfalls [8, 9]. Concurrently, reasoning-centric LVLMs show rapid progress: *LLaVA-CoT* introduces staged, autonomous visual CoT and improves across reasoning-heavy suites [46]; *Mulberry* equips MLLMs with o1-like step-by-step reasoning and reflection via a collective MCTS procedure [49]; *InternVL 3.5* reports strong reasoning results across MMMU/MathVista with cascade RL [19, 41]; and *Qwen3-VL* releases Instruct/Thinking variants with broad coverage and improved visual reasoning [29]. We investigate these families to quantify where components changes translate into visual reasoning gains.

2.3. LVLM Analysis

Complementary work analyzes how LVLMs perceive and ground visual content: [7] reveal visual-token–specialized attention heads whose concentration correlates with visual understanding; [22] show that a small subset of “localiza-

Model	Variants [†]	LLM backbone	Vision encoder	Connector	Image tokens
InternVL3.5-4B	instruct, COT	Qwen3 4B	InternViT-300M (ViT/14)	MLP projector	$\lceil H \times W / 28^2 \rceil$ DHR TILING
InternVL3.5-8B	instruct, COT	Qwen3 8B	InternViT-300M (ViT/14)	MLP projector	$\lceil H \times W / 28^2 \rceil$ DHR TILING
Qwen3-VL-4B	instruct, thinking	Qwen3 4B	Qwen3VLVision (ViT/16)	DeepStack	$\lceil H \times W / 32^2 \rceil$ 2x2 MERGE
Qwen3-VL-8B	instruct, thinking	Qwen3 8B	Qwen3VLVision (ViT/16)	DeepStack	$\lceil H \times W / 32^2 \rceil$ 2x2 MERGE
Qwen3-VL-32B	instruct, thinking	Qwen3 32B	Qwen3VLVision (ViT/16)	DeepStack	$\lceil H \times W / 32^2 \rceil$ 2x2 MERGE

Table 1. **Model comparison.** **Image tokens:** *Qwen3-VL* uses an effective stride of 32 (ViT/16 with 2×2 token merging), yielding $\lceil (H \times W) / 32^2 \rceil$ tokens for an image (e.g., $1024 \times 1024 \rightarrow 1024$ tokens). *InternVL3.5* uses ViT/14 features with $4 \times$ pixel unshuffle and **DHR** (Dynamic High-Resolution) tiling: the image is split into 448×448 tiles; each tile contributes ≈ 256 tokens after compression, and an optional global thumbnail adds $+256$. For a 1024×1024 image, $\lceil 1024 / 448 \rceil = 3$ per side $\Rightarrow 3 \times 3 = 9$ tiles, so $9 \times 256 = 2304$ tokens (optionally $+256$). **DeepStack** (*Qwen3-VL*) denotes a multi-level ViT feature stacking/fusion module with 2×2 token merging that reduces the visual token grid by $4 \times$ before the LLM. **Variants:** *instruct* vs. *COT/thinking*. Here, *COT* means the model is *prompted* to reason and may or may not emit a thinking trace. In *Qwen3-VL*, *thinking* mode injects a `<think>` token in the prompt, so a thinking trace is consistently generated. In total, we compare 8 distinct model checkpoints with 10 variants in total.

tion heads” suffices for competitive training-free grounding; and [18, 36] revisit multimodal positional encodings, distilling design rules that improve grounding and video understanding. Object-level hallucination is traced to specific architectural and optimization factors with targeted mitigations [21]; an inference-time head-suppression strategy links hallucination to low image-attending heads and reduces errors with minimal latency [31]; and VLM-LENS provides a toolkit for probing intermediate layers and standardizing interpretability analyses for open-source VLMs [32], informing our diagnostics separating perception from reasoning.

3. Analysis

In this section, we first describe our experimental setup, including the datasets, models, decoding strategies, and token budgets. We then present our empirical findings on the effects of *Thinking* and its impact on visual reasoning.

Dataset and Models. We adopt MMMU_{val} as our analysis benchmark because of its diversity and its widespread use in the LVLM literature; its 30 categories provide a rich opportunity to investigate generalization, robustness, and model strengths and failure modes [51]. We focus on two leading open-source VLM families and their variants, rank top-performing open-source systems on the MMMU_{val} leaderboard [1]. As shown in Table 1, both are built upon Qwen3 LLM backbones, allowing controlled comparisons across three key dimensions: (i) vision encoder architectures (InternViT vs. Qwen3VLVision), (ii) connector architectures (MLP vs. DeepStack), and (iii) reasoning modes. This alignment makes the families well-suited for representative and systematic within-family comparison [1, 2, 42, 51], and, to the best of our knowledge, there are currently no publicly available visual CoT controllers tailored to their “thinking” modes, making decoding-time control a practical way to improve performance without modifying model.

Multiple-pass decoding. We adopt a multi-sample evaluation setting with 10 sampled reasoning paths per item. This follows evidence that sampling diverse answers and

Evaluator	Year	Passes	Instruct	Reasoning
LMMs-Eval [52]	2024	1	128	128
EvalScope [15, 27]	2024	1	512	512
VLMevalKit [13]	2024	1	512	512
NeMo [28]	2025	1	2,048	2,048
VHELM [23]	2024	1	4,096	4,096
Vals.ai [38]	2025	1	8,192	16,384
CombiGraph-Vis [26]	2025	8	–	–
MIRA [58]	2025	8	8,192	16,384
Ours	2025	10	16,384	32,768

Table 2. Maximum *output* tokens for MMMU_{val} across widely used toolkits and recent CoT-style benchmarks, and the number of sampling passes used per question. We intentionally set a substantially larger budget and more passes to reduce truncation and enable longer reasoning chains.

marginalizing across them improves multi-step reasoning [44] and aligns with recent work on visual reasoning and CoT prompting [26, 58]. While prior work [26, 58] typically uses 8 passes, we use 10 for consistency across models and a stronger assessment of answer stability. Temperature and top_p follow standard MMMU_{val} leaderboard, varying only random seeds [27, 52], whereas common evaluation toolkits default to single-sample decoding [13, 27, 52]. Further sampling details are provided in the appendix.

Token budgets. Compared to commonly used evaluators, we employ substantially larger output-token budgets. Specifically, we allocate 16,384 tokens for *Instruct* and 32,768 for *Reasoning*, reducing truncation and enabling fully articulated solution chains when beneficial [27, 52]. This design helps ensure that performance differences are not confounded by output-length constraints (Table 2).

3.1. Will Thinking Help?

We examine two thinking paradigms for improving reasoning: thinking in **breadth** (sampling more candidates, i.e., $\text{pass}@k$) and **depth** (explicit reasoning). The $\text{pass}@k$ curves (Fig. 1) characterize how performance scales with additional samples, while the mean pass accuracy boxplots (Fig. 3) summarize the overall accuracy and variability of each model family and its thinking-enabled variant.

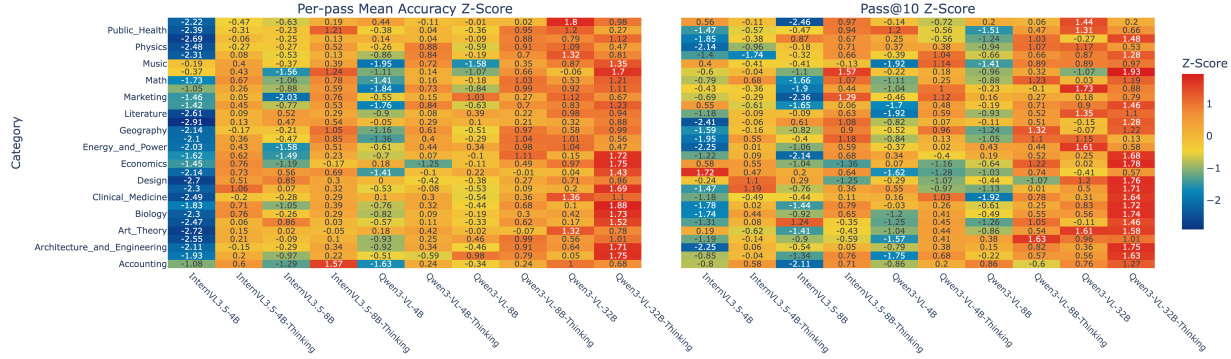


Figure 2. Category-level performance heatmaps showing z-scored accuracy across disciplines for all models and their thinking variants. Left: mean accuracy z-scores; right: Pass@10 z-scores under extensive sampling. Warmer colors indicate categories where a model performs above the global average, while cooler colors highlight relative weaknesses.

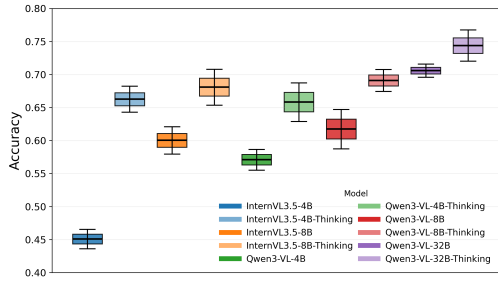


Figure 3. Mean Pass@k accuracy on $MMMU_{val}$ for each vision-language model and its corresponding “Thinking” variant. Boxplots summarize variation across evaluation runs, where higher medians and tighter interquartile ranges indicate stronger and more stable performance, highlighting systematic differences between standard and Thinking modes.

Thinking in Breadth. Increasing k monotonically improves accuracy for every model: the $\text{pass}@k$ curves in Fig. 1 steadily rise, indicating that a substantial portion of errors can be corrected with just a few extra attempts. The gains are steep from $k = 2$ to $k = 6$ and then clearly taper off for $k \geq 8$, revealing diminishing returns from pure sampling-based search. Smaller models benefit disproportionately from larger k : their single-sample accuracy lags behind, but additional samples give them more chances to land on a successful reasoning trajectory. With sufficient sampling, weaker models partially close the gap to much larger ones without explicit reasoning. For example, at high k the InternVL3-4B curve moves noticeably closer to

Qwen3-VL-32B (instruct), even though a performance margin remains. In some regimes ($k \geq 6$), a smaller *thinking-enabled* model can overtake a larger instruct-only model, showing that increasing k can substitute for raw parameter count when latency and cost budgets allow.

Thinking in Depth. Across all model sizes and values of k , the thinking variants consistently outperform their instruct counterparts in both Fig. 1 and Fig. 3. The relative gains are most pronounced for smaller models and gradually narrow as capacity increases. Thinking improves the *quality* of each sampling rather than removing the need for multiple samples: for a fixed target accuracy, thinking variants typically achieve it at a lower k than their non-thinking baselines. The standard-deviation bands in Fig. 1 and the spread of the boxplots in Fig. 3 are generally smaller for thinking variants, suggesting more stable reasoning traces and fewer catastrophic failures across random seeds and prompts. Thinking allows smaller models to challenge, and in some cases surpass substantially larger instruct-only models. For instance, Qwen3-VL-4B-thinkink can match or exceed InternVL3.5-8B-instruct under comparable sampling budgets. At the 8B scale, the two families largely converge once thinking is enabled: with sufficient capacity and visual modeling, additional parameter scaling yields only modest further gains, especially at higher k .

Yes, thinking helps. Reasoning raises baseline accuracy and reduces variance, while sampling efficiently recovers near-miss solutions. Effective multimodal reasoning benefits from both: higher-quality single-sample chains of thought and enough samples to explore alternatives. Nevertheless, there remain cases where even combining breadth and depth fails to resolve the problem as shown in Fig. 4. We show additional examples are provided in the appendix

3.2. Does Thinking Lead in All Categories?

Figure 2 reports per-category Z-scores for two complementary views: **Depth** (left), the mean accuracy over 10 independent passes (single-sample reliability), and **Breadth**

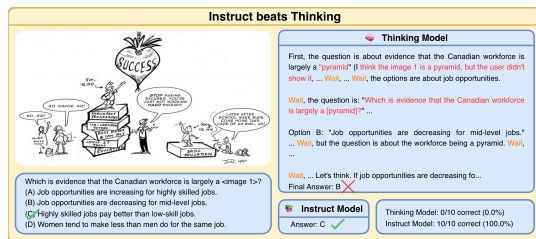


Figure 4. An example where the 32B thinking model fails on all 10 passes, while the instruct model answers correctly using 1 token.



Figure 5. Token footprint of instruct vs. thinking across difficulty and scale. Boxplots show the distribution of total generated tokens per question, split by correctness (correct vs. wrong), model family (InternVL3.5 vs. Qwen3-VL), size (4B/8B/32B), and difficulty (Easy/Medium/Hard). The top panel reports *Instruct* models, while the bottom reports *Thinking* variants. Thinking consistently inflates token usage relative to instruct—especially on medium and hard questions and on failures—illustrating the compute overhead of deliberate reasoning. At larger scales (e.g., 32B), correct thinking traces tend to be shorter than for smaller models at the same difficulty, suggesting more efficient reasoning with increased capacity.

(right), the aggregated accuracy under sampling (pass@10), i.e., the probability that at least one of k samples is correct. Within each category, scores are standardized across all model variants (warmer = better relative to peers), and both panels share the same color scale.

Reasoning-centric domains favor depth for small/mid models. In numerically intensive categories such as Physics, Math, Engineering, Chemistry, Biology, Clinical/Diagnostics, and computation-heavy Finance, *Thinking* substantially warms the InternVL3.5-4B column in Depth relative to its *Instruct* baseline, and often also improves Qwen3-VL at 8B and 32B. This mirrors the global trend from Fig. 3/1: explicit reasoning makes each pass more reliable, so fewer samples are needed to reach a given accuracy. The effect is uneven across capacities and families, for instance, InternVL3.5-8B-*Thinking* regresses on some STEM/business rows, suggesting that depth helps most when capacity can support coherent chains.

Recognition centric categories often prefer concise Instruct. In Literature, History, Art/Art_Theory, Music, and several social-science categories (Sociology, Public_Health, Psychology), the Depth heatmap does not show a systematic warm shift for *Thinking*, and in Breadth the *Instruct* variants at 8B and 32B are frequently as warm as, or warmer than, their *Thinking* counterparts. Here the task leans more on recognition and retrieval from priors than on multi-step deduction; longer chains mainly introduce noise, which extra sampling does not convert into more correct alternatives.

3.3. How Does Thinking Perform?

Across all difficulties (Easy/Medium/Hard), the top row of Fig. 5 shows that total tokens are governed far more by *language* capacity than by the vision stack or family differences. Within each difficulty group, moving from 4B → 8B → 32B systematically shortens responses and tight-

ens the boxplots for both families, under both *Instruct* and *Thinking*. We include key observations below and defer further discussion to the appendix.

Capacity-driven concision is family-invariant. Despite architectural differences in the visual front-end (InternViT/14 with tiling vs. Qwen3-VL’s ViT/16 tokenization), the token distributions for the two families are remarkably similar when matched by scale. For each Easy/Medium/Hard column, the 32B variants sit lowest and most concentrated, 8B is in the middle, and 4B is highest with the heaviest tails, in both panels. The “token economy” is therefore largely a function of language-side capacity rather than encoder or connector design.

Deliberation cost is highest where it helps least. Comparing the *Instruct* and *Thinking* panels, enabling reasoning roughly doubles the median token count on Easy questions at 4B and 8B, yet these are precisely the regimes where Fig. 1 shows only modest accuracy gains. On Hard questions, the multiplier is still present but less wasteful: longer chains are more likely to correspond to useful steps, especially for the smaller models. Overall, the overhead factor of *Thinking* is largest for easy problems and small variants.

Equivalence across difficulty, capacity, and mode. The figure implicitly traces budget frontiers: for a fixed mode, moving one step up in capacity (4B → 8B or 8B → 32B) often reduces the median token count by a similar amount to moving one step down in difficulty (Hard → Medium → Easy), and switching from *Thinking* to *Instruct* can yield a comparable saving. In practice, this enables budget-aware routing: a Hard query on a small model with *Thinking* can have a similar token footprint to a Medium query on a mid-sized model or an Easy query on a large model under *Instruct*, allowing systems to trade off capacity, difficulty.

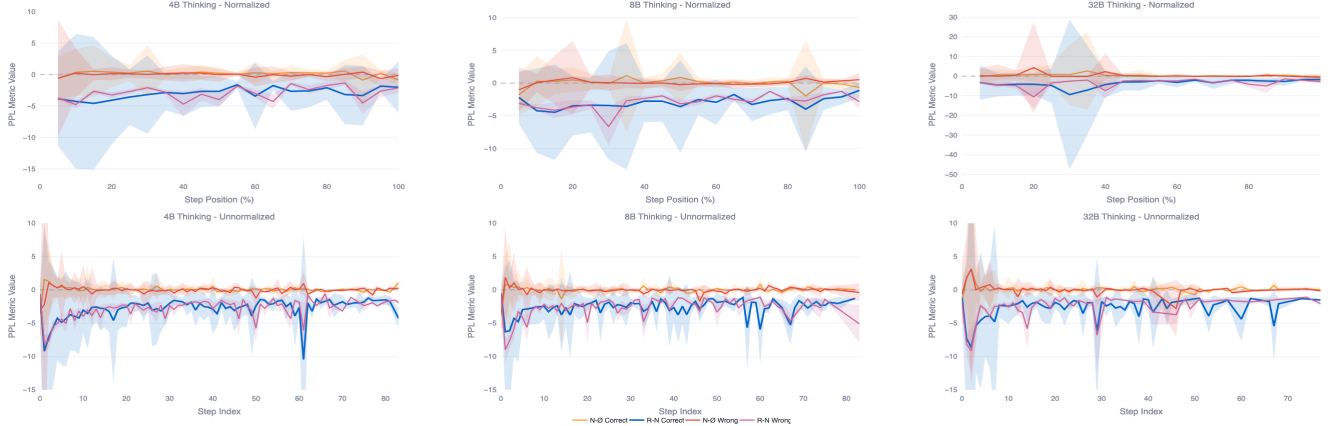


Figure 6. Token-level ΔPPL dynamics over the course of thinking for 4B, 8B, and 32B models. Top: traces normalized to a common 0–100% step position. Bottom: unnormalized step index. Blue and magenta curves correspond to the R – N contrast for correct and wrong answers, respectively, while orange and red show N – \emptyset . The y -axis shows the change in per-token perplexity (ΔPPL): negative values (e.g., -10) mean the visual condition makes the next token much easier to predict, effectively narrowing down the model’s plausible choices, whereas positive values (e.g., $+10$) mean it makes the token harder to predict, broadening or diffusing the set of plausible continuations.

4. Improvement

In Sec.3, we show that *more thinking is not always better*: across model size, wrong answers often use as many or more tokens than correct ones, with small models in particular producing long, low-utility chains (“long-wrong”) on easy and medium items. These observations motivate *adaptive* control over when and how to think, conditioned on both uncertainty and grounding. Moreover, Sec.3 exposes systematic failures on certain MMMU_{val} categories, such as Sociology, where the model drifts into ungrounded textual speculation instead of using the image. Building on these diagnostics, we propose a training-free decoding strategy based on a token-level probe that (i) detects when the chain of thought enters a visually uncertain regime, (ii) triggers visual lookbacks online during streaming generation.

4.1. Token-Level Visual Sensitivity Probe

Following the step-decomposition protocol of [34], we run each model in thinking mode and decompose its decoded trace into word-level steps. Let the input question be x , the image be I , and the thinking trace consist of tokens

$$y_{1:S} = (y_1, y_2, \dots, y_S).$$

For each step $s \in \{1, \dots, S\}$ we evaluate the model under three visual contexts: *Real image* $c = R$: the original image I ; *Noise image* $c = N$: a visually mismatched image of the same resolution, e.g., Gaussian noise that carries no semantic information about x (we deliberately use synthetic noise rather than a real but unrelated image: a mismatched real image still carries rich semantic content, and LVLMs may attempt to align their reasoning with whatever objects or text it contains, confounding the probe’s interpretation of ‘no useful visual evidence’). Noise, by contrast, provides a

structurally valid but semantically empty control); *No image* $c = \emptyset$: no visual tokens are provided.

Because the decoder is autoregressive, we can compute per-step perplexity under each context to see how the image’s presence and content affect token prediction:

$$\text{PPL}_c(s) = \exp(-\log p_\theta(y_s | x, I_c, y_{<s})), \quad (1)$$

where $c \in \{R, N, \emptyset\}$. We then form two difference scores:

$$\Delta_{\text{content}}(s) = \text{PPL}_R(s) - \text{PPL}_N(s), \quad (2)$$

$$\Delta_{\text{presence}}(s) = \text{PPL}_N(s) - \text{PPL}_\emptyset(s). \quad (3)$$

Intuitively, $\Delta_{\text{content}}(s)$ measures how much the *correct* image content helps at step s . In contrast, $\Delta_{\text{presence}}(s)$ isolates the effect of merely *having any image* present: a large magnitude means that presence of visual tokens helps.

We use the two contrast axes jointly but for different purposes. $\Delta_{\text{presence}}(s)$ acts as a probe for visually uncertain steps: positions with large $|\Delta_{\text{presence}}(s)|$ but small $|\Delta_{\text{content}}(s)|$ behave like generic “there is an image here” reactions—highly sensitive to visual tokens but not to specific content. By aggregating such steps across traces, we mine local n -grams whose usage consistently coincides with this regime and augment them with reflection-style uncertainty markers (e.g., “hmm”, “wait”) from prior work [16, 34], yielding a compact lexical pause-phrase vocabulary that can be matched online without recomputing perplexities.

In contrast, $\Delta_{\text{content}}(s)$ highlights strongly image-dependent reasoning: as Fig. 6 shows, the content contrast is more negative for correctly answered examples than for wrong ones across most of the trajectory and model sizes, indicating that successful solutions maintain sustained visual grounding rather than relying on a single early glance. In the unnormalized plots, this appears as frequent sharp

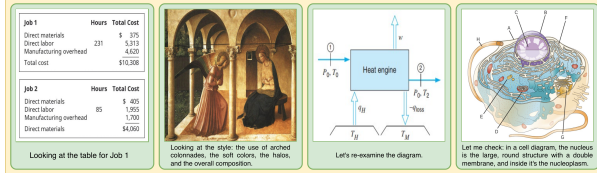


Figure 7. Examples of mined “lookback” sentences with strong dependence on the image. Each panel shows a problem image from a different domain with a reflection sentence that explicitly directs the model to re-examine task-relevant visual details.

dips in the correct ($R - N$) curves but fewer, shallower dips for wrong traces, indicating that successful solutions are marked by repeated, localized lookbacks to image content throughout the chain of thought. We leverage this cue to mine *lookback phrases*: multi-token templates that consistently co-occur with highly negative $\Delta_{\text{content}}(s)$ in correctly solved examples. These phrases, shown in Fig. 7, explicitly prompt the model to re-examine task-relevant visual details. We mine uncertainty phrases on the same validation set used for the visual probe (which serves as ‘pseudo ground truth’), filtering high-scoring tokens and searching them across 10 sampled passes, where we find an 89% alignment between mined phrases and high-uncertainty positions; we further observe similar patterns across the five additional datasets we evaluate, suggesting these phrases capture intrinsic LLM behavior rather than dataset artifacts, with full details provided in the appendix.

4.2. Lookback-When-Uncertain Decoding

At test time, we implement *lookback-when-uncertain* as a lightweight controller over standard autoregressive decoding. Let \mathcal{P} denote the pause-phrase vocabulary (mined from steps with large $|\Delta_{\text{presence}}(s)|$ and small $|\Delta_{\text{content}}(s)|$, plus uncertainty markers from [16, 34]), and let \mathcal{L} denote the set of lookback templates (extracted from steps with highly negative $\Delta_{\text{content}}(s)$ in correct traces). During streaming, the controller operates as: At step $t + 1$ we sample $y_{t+1} \sim p_{\theta}(\cdot | x, I, y_{\leq t})$ and set

$$y'_{1:t+1} = \begin{cases} y_{1:t} \| y_{t+1} \| \ell, & \text{if } \neg \text{ans}(t), \neg \text{trig}(t), \\ & \text{suffix}_L(y_{1:t+1}) \in \mathcal{P}, \\ y_{1:t} \| y_{t+1}, & \text{otherwise,} \end{cases}$$

where $\|$ denotes concatenation, $\ell \in \mathcal{L}$ is a lookback phrase (e.g., “Looking back at the image, ...”), suffix_L returns the length- L suffix of the trace, $\text{trig}(t)$ indicates a lookback was triggered in the last L thinking tokens, and $\text{ans}(t)$ that the model has entered the final-answer segment.

Intuitively, whenever the recent context contains a pause phrase from \mathcal{P} and the model is still in the thinking phase, we immediately append a lookback template from \mathcal{L} , forcing an explicit re-consultation of the image before reasoning proceeds. To prevent degeneration, we allow at most one lookback trigger within any window of L thinking tokens

and disable further triggers once the final-answer phase starts. All heavy computation (estimating $\Delta_{\text{presence}}(s)$ and $\Delta_{\text{content}}(s)$ and mining \mathcal{P}, \mathcal{L}) is done offline. At inference time, the controller reduces to efficient n -gram matching over streamed tokens plus occasional insertion of short lookback prompts, making it compatible with token-by-token streaming and avoiding any perplexity estimation.

4.3. Parallel Lookback Sampling

The same probe can also help choose *which* visual reasoning branch to follow. When a lookback is triggered at step s , we sample M short continuations of horizon H after injecting $\phi: y_{s:s+H}^{(m)}$, $m = 1, \dots, M$. For each branch we compute an aggregate visual helpfulness score

$$\mathcal{V}^{(m)} = -\frac{1}{H} \sum_{t=s}^{s+H-1} \Delta_{\text{content}}^{(m)}(t), \quad (4)$$

so that larger $\mathcal{V}^{(m)}$ corresponds to trajectories where the real image consistently reduces the loss compared to noise. We then select the branch with maximal $\mathcal{V}^{(m)}$ and continue decoding from its state. Because lookback events are rare and localized, this parallel lookback sampling adds only a small overhead to the total token budget, yet substantially increases the chance that at least one branch is tightly grounded in the image. This gives a compute-efficient mechanism: smaller models gain robustness by exploring multiple grounded branches, while larger models use lookback more sparingly, primarily to correct the hardest cases. Due to page limits, we report in the appendix additional experiments using an online perplexity-based controller, and we find that its effect is very similar to our phrase-based triggers, indicating that lightweight lexical cues are sufficient and the practical gap between the probe and the deployed controller is minor. We provide a more detailed compute and latency characterization in the appendix, including wall-clock and throughput comparisons under different configurations, showing that our method improves the accuracy–compute trade-off with modest overhead.

4.4. Baselines

We compare against three recent *training-free* adaptive reasoning methods, all developed for text-only CoT and thus complementary to our vision-language setting. DEER (Dynamic Early Exit in Reasoning) [48] proposes a confidence-based early-exit rule over reasoning tokens. DeepConf (Deep Think with Confidence) [16] uses token-level confidence to prune and vote over multiple CoT traces. REFRAIN [34] introduces a discriminator-based early-stopping policy with instance-wise threshold adaptation. Together, these baselines represent the current state of training-free adaptive CoT decoding on the language side, and we use them here as strong text-only control baselines to test whether generic early-exit signals transfer to LLMs.

Size	Method	overall		Finance		Sociology		Physics		DLM		EP		Design	
		Pass@1	%Tokens												
4B	Original	67.0	100.0	65.3	100.0	60.7	100.0	65.7	100.0	52.0	100.0	63.0	100.0	59.3	100.0
	DEER	53.3	40.0	53.3	36.7	46.7	40.0	56.7	36.7	43.3	40.0	50.0	36.7	50.0	40.0
	Deepconf	63.3	76.7	66.7	76.7	56.7	76.7	66.7	76.7	50.0	73.3	66.7	76.7	60.0	76.7
	REFRAIN	63.3	73.3	63.3	63.3	60.0	76.7	66.7	80.0	53.3	76.7	66.7	76.7	63.3	63.3
8B	Ours (lookback)	69.7(+2.7)	57.2(-42.8)	68.5(+3.2)	59.4(-40.6)	62.6(+1.9)	56.3(-43.7)	67.2(+1.5)	59.1(-40.9)	57.0(+5.0)	57.8(-42.2)	67.5(+4.5)	56.9(-43.1)	61.6(+2.3)	59.3(-40.7)
	Ours (+sampling)	73.0(+6.0)	59.5(-40.5)	71.8(+6.5)	55.0(-45.0)	64.3(+3.6)	58.3(-41.7)	71.0(+5.3)	53.0(-47.0)	58.3(+6.3)	58.3(-41.7)	72.3(+9.3)	55.0(-45.0)	62.0(+2.7)	55.2(-44.8)
	Original	70.3	100.0	69.0	100.0	63.3	100.0	71.7	100.0	59.7	100.0	67.3	100.0	59.0	100.0
	DEER	60.0	40.0	56.7	40.0	53.3	43.3	60.0	40.0	50.0	43.3	60.0	40.0	50.0	40.0
32B	Deepconf	66.7	80.0	66.7	76.7	63.3	80.0	66.7	80.0	56.7	80.0	70.0	80.0	56.7	80.0
	REFRAIN	70.0	83.3	66.7	83.3	60.0	83.3	70.0	83.3	60.0	83.3	66.7	83.3	56.7	83.3
	Ours (lookback)	73.0(+2.7)	62.1(-37.9)	76.7(+7.7)	60.2(-39.8)	65.3(+2.0)	65.0(-35.0)	76.7(+5.0)	60.9(-39.1)	64.3(+4.6)	62.3(-37.7)	75.1(+7.8)	61.2(-38.8)	63.7(+4.7)	64.0(-36.0)
	Ours (+sampling)	74.2(+3.9)	63.0(-37.0)	74.1(+5.1)	58.0(-42.0)	68.8(+5.5)	63.5(-36.5)	74.1(+2.4)	59.0(-41.0)	64.9(+5.2)	67.3(-32.7)	75.8(+8.5)	63.3(-36.7)	61.0(+2.0)	64.8(-35.2)
	Ours (lookback)	81.7(+6.4)	66.2(-33.8)	72.5(+5.5)	61.4(-38.6)	70.6(+2.3)	62.1(-37.9)	72.5(+2.2)	64.0(-36.0)	71.1(+5.4)	65.2(-34.8)	73.3(+2.3)	65.8(-34.2)	80.1(+2.4)	61.3(-38.7)
	Ours (+sampling)	79.2(+3.9)	70.3(-29.7)	73.1(+6.1)	65.3(-34.7)	71.3(+3.0)	63.0(-37.0)	76.5(+6.2)	61.0(-39.0)	72.0(+6.3)	66.3(-33.7)	77.3(+6.3)	63.5(-36.5)	84.2(+6.5)	61.5(-38.5)

Table 3. MMMU_{val} performance (Pass@1, token usage percentage) on overall and selected categories for our methods on Qwen3-VL models. Deltas are differences w.r.t. the corresponding Original. DLM = Diagnostics and Laboratory Medicine, EP = Energy and Power.

Size	Model	MMBench	MMStar	MathVista	MathVision	MathVerse
4B	Original	86.7	73.2	79.5	60.0	75.2
	Ours (lookback)	89.5(+2.8)	75.0(+1.8)	84.3(+4.8)	64.2(+4.2)	77.2(+2.0)
	Ours (+sampling)	88.2(+1.5)	75.7(+2.5)	85.0(+5.5)	65.5(+5.5)	78.7(+3.5)
	Original	87.5	75.3	77.2	62.7	77.7
8B	Ours (lookback)	88.7(+1.2)	78.5(+3.2)	79.4(+2.2)	67.9(+5.2)	78.9(+1.2)
	Ours (+sampling)	89.8(+2.3)	79.6(+4.3)	79.7(+2.5)	68.3(+5.6)	79.9(+2.2)
	Original	90.8	79.4	83.8	70.2	82.6
	Ours (lookback)	93.6(+2.8)	81.2(+1.8)	85.6(+1.8)	72.0(+1.8)	84.4(+1.8)
32B	Ours (+sampling)	93.9(+3.1)	82.5(+3.1)	85.9(+2.1)	73.3(+3.1)	84.7(+2.1)

Table 4. Accuracy (%) on selected benchmarks for Qwen3-VL Thinking models across different sizes, comparing the Original

4.5. Results

To assess generality, we evaluate on MMMU_{val} and five established vision–language benchmarks. MMBench [24] and MMStar [10] probe broad multimodal capabilities, while MathVista [25], MathVision [39], and MathVerse [54] focus on visual mathematical reasoning. Detailed MMMU_{val} results are reported in Tab. 3, and cross-benchmark results in Tab. 4. On MMMU_{val} , our method consistently improves both accuracy and efficiency over the original Qwen3-VL Thinking models across all sizes (Tab. 3). For example, on the 4B model our lookback variant raises Pass@1 from 59.3% to 61.6% while using only about 57% of the original tokens, and the sampling variant pushes Pass@1 to around 62.0% with a similar or slightly larger reduction in token usage. At 8B and 32B, we observe comparable overall gains (roughly +2–+3 absolute points) while cutting token usage by about one third. These improvements are particularly pronounced in specialist domains such as Diagnostics and Laboratory Medicine or Energy and Power, where Pass@1 can improve by up to +5–+6.5 points with 35–40% fewer tokens. Taken together, these results indicate that our method shifts the Pareto frontier on MMMU_{val} : for a fixed token budget we achieve higher accuracy, and for a fixed accuracy target we require substantially fewer tokens.

The cross-benchmark results in Tab. 4 show that these

gains generalize beyond MMMU_{val} . Across MMBench and MMStar, both variants consistently outperform the original models at all scales, typically improving accuracy by a few absolute points even when baselines are already strong. On the math-focused benchmarks—MathVista-mini, MathVision-full, and MathVerse-mini—the benefits are larger: at 4B and 8B we obtain gains of roughly +4–+6 points on MathVista and MathVision and +2–+3.5 on MathVerse, with smaller but still positive gains at 32B. This pattern suggests that our approach particularly strengthens multi-step visual mathematical reasoning while also yielding robust improvements on multimodal understanding.

Comparing the two variants, the lookback strategy already offers a favorable accuracy–efficiency trade-off and is attractive when deterministic behavior is preferred. The additional sampling step further boosts performance, especially on math-heavy benchmarks and difficult MMMU_{val} categories, at a modest extra token cost relative to lookback alone. Overall, our approach provides a simple, plug-and-play enhancement to Qwen3-VL Thinking models that scales well with model size: it consistently yields higher accuracy—often by several absolute points—while reducing token usage by roughly 35–45%. The appendix includes additional qualitative examples illustrating when lookback helps (e.g., correcting missed visual details) and when it can occasionally hurt.

5. Conclusion

We find that more “vanilla thinking” is not always better for LVLMs: long chains help only in certain settings and often produce overlong, weakly grounded reasoning on easy or recognition-heavy tasks. To fix this, we propose a training-free, uncertainty-guided lookback that injects short, image-focused prompts only when chains drift, using extra compute only where visual reasoning helps. Across diverse visual benchmarks, this adaptive decoding improves accuracy over strong baselines while often using fewer tokens.

References

[1] Mmmu (val) leaderboard snapshot. <https://mumu-benchmark.github.io/>, 2025. Lists Qwen3-VL 32B “Thinking” at the top among open-source models at the time of access. 3

[2] Qwen3-vl: Model and documentation. <https://github.com/QwenLM/Qwen3-VL>, 2025. 3

[3] Jiwei Bai et al. Qwen-vl: A versatile vision-language model for understanding, localization, text reading, and beyond. *arXiv preprint arXiv:2308.12966*, 2023. 2

[4] Shen Bai et al. Qwen2.5-vl technical report. *arXiv preprint arXiv:2502.13923*, 2025. 2

[5] Jing Bi, Jiebo Luo, and Chenliang Xu. Procedure planning in instructional videos via contextual modeling and model-based policy learning. In *Proceedings of the IEEE/CVF International Conference on Computer Vision (ICCV)*, pages 15611–15620, 2021. 2

[6] Jing Bi, Junjia Guo, Yunlong Tang, Jingyuan Li, Xinjie Liu, and Chenliang Xu. Verify: A benchmark of visual explanation and reasoning for investigating multimodal reasoning fidelity. *arXiv preprint arXiv:2503.11557*, 2025. 2

[7] Jing Bi, Junjia Guo, Yunlong Tang, Lianggong Bruce Wen, Zhang Liu, Bingjie Wang, and Chenliang Xu. Unveiling visual perception in language models: An attention head analysis approach. In *Proceedings of the IEEE/CVF Conference on Computer Vision and Pattern Recognition (CVPR)*, pages 4135–4144, 2025. Open Access. 2

[8] Jing Bi, Susan Liang, Xiaofei Zhou, Pinxin Liu, Junjia Guo, Yunlong Tang, Luchuan Song, Chao Huang, Guangyu Sun, Jinxi He, Jiarui Wu, Shu Yang, Daoan Zhang, Chen Chen, Lianggong Bruce Wen, Zhang Liu, Jiebo Luo, and Chenliang Xu. Why reasoning matters? a survey of advancements in multimodal reasoning. *arXiv preprint arXiv:2504.03151*, 2025. 2

[9] Jing Bi, Guangyu Sun, Ali Vosoughi, Chen Chen, and Chenliang Xu. Diagnosing visual reasoning: Challenges, insights, and a path forward. *arXiv preprint arXiv:2510.20696*, 2025. 2

[10] Lin Chen, Ruili Zhang, Yuxin Zhou, et al. Are we on the right way for evaluating large vision-language models? *arXiv preprint arXiv:2403.20330*, 2024. NeurIPS 2024 (Datasets and Benchmarks Track). 8

[11] Yanda Chen, Yongqiang Wang, Xiang Zhou, Yanzheng Cai, Tong Yu, Sen Li, and Xiaowei Huang. Reasoning models don’t always say what they think. *arXiv preprint arXiv:2505.05410*, 2025. 2

[12] Jiahao Cheng, Tiansheng Su, Jia Yuan, Guoxiu He, Jiawei Liu, Xinqi Tao, Jingwen Xie, and Huaxia Li. Chain-of-thought prompting obscures hallucination cues in large language models: An empirical evaluation. *arXiv preprint arXiv:2506.17088*, 2025. 2

[13] Haodong Duan, Xinyu Fang, Junming Yang, Xiangyu Zhao, Yuxuan Qiao, Mo Li, Amit Agarwal, Zhe Chen, Lin Chen, Yuan Liu, Yubo Ma, Hailong Sun, Yifan Zhang, Shiyin Lu, Tack Hwa Wong, Weiyun Wang, Peiheng Zhou, Xiaozhe Li, Chaoyou Fu, Junbo Cui, Jixuan Chen, Enxin Song, Song

Mao, Shengyuan Ding, Tianhao Liang, Zicheng Zhang, Xiaoyi Dong, Yuhang Zang, Pan Zhang, Jiaqi Wang, Dahua Lin, and Kai Chen. Vlmevalkit: An open-source toolkit for evaluating large multi-modality models. *arXiv preprint arXiv:2407.11691*, 2024. 3

[14] Scott Emmons et al. When chain of thought is necessary, language models struggle to evade monitors. *arXiv preprint arXiv:2507.05246*, 2025. 1

[15] EvalScope Team. Evalscope documentation — cli parameters. <https://evalscope.readthedocs.io/>, 2025. Default `max_new_tokens=512`. 3

[16] Yichao Fu, Xuewei Wang, Yuandong Tian, and Jiawei Zhao. Deep think with confidencebib. *arXiv preprint arXiv:2508.15260*, 2025. 2, 6, 7

[17] Yushi Hu et al. Visual sketchpad: Sketching as a visual chain of thought for multimodal language models. *arXiv preprint arXiv:2406.09403*, 2024. 2

[18] Jie Huang, Xuejing Liu, Sibo Song, Ruibing Hou, Hong Chang, Junyang Lin, and Shuai Bai. Revisiting multimodal positional encoding in vision–language models. *arXiv preprint arXiv:2510.23095*, 2025. 3

[19] InternVL Team. Internvl3.5: Advancing open-source multimodal models in versatility, reasoning, and efficiency. <https://internvl.github.io/blog/2025-08-26-InternVL-3.5/>, 2025. Release announcement. 2

[20] Dongzhi Jiang, Renrui Zhang, Ziyu Guo, Yanwei Li, Yu Qi, Xinyan Chen, Liuhui Wang, Jianhan Jin, Claire Guo, Shen Yan, Bo Zhang, Chaoyou Fu, Peng Gao, and Hongsheng Li. Mme-cot: Benchmarking chain-of-thought in large multimodal models for reasoning quality, robustness, and efficiency. *arXiv preprint arXiv:2502.09621*, 2025. 2

[21] Lingjing Jing et al. A comprehensive analysis for visual object hallucination in large vision-language models. *arXiv preprint arXiv:2505.01958*, 2025. 3

[22] Seil Kang, Jinyeong Kim, Junhyeok Kim, and Seong Jae Hwang. Your large vision-language model only needs a few attention heads for visual grounding. In *Proceedings of the IEEE/CVF Conference on Computer Vision and Pattern Recognition (CVPR)*, pages 9339–9348, 2025. 2

[23] Percy Liang, Rishi Bommasani, Tony Lee, Dimitris Tsipras, Dilara Soylu, Michihiro Yasunaga, Yian Zhang, Deepak Narayanan, Yuhuai Wu, Ananya Kumar, Benjamin Newman, Binhang Yuan, Bobby Yan, Ce Zhang, Christian Alexander Cosgrove, Christopher D Manning, Christopher Re, Diana Acosta-Navas, Drew Arad Hudson, Eric Zelikman, Esin Durmus, Faisal Ladhak, Frieda Rong, Hongyu Ren, Huaxiu Yao, Jue WANG, Keshav Santhanam, Laurel Orr, Lucia Zheng, Mert Yuksekgonul, Mirac Suzgun, Nathan Kim, Neel Guha, Niladri S. Chatterji, Omar Khattab, Peter Henderson, Qian Huang, Ryan Andrew Chi, Sang Michael Xie, Shibani Santurkar, Surya Ganguli, Tatsunori Hashimoto, Thomas Icard, Tianyi Zhang, Vishrav Chaudhary, William Wang, Xuechen Li, Yifan Mai, Yuhui Zhang, and Yuta Koreeda. Holistic evaluation of language models. *Transactions on Machine Learning Research*, 2023. Featured Certification, Expert Certification. 3

[24] Yuxin Liu, Haodong Duan, Zhenfei Wang, et al. MMBench:

Is your multi-modal model an all-around player? *arXiv preprint arXiv:2307.06281*, 2023. 8

[25] Pan Lu, Mohit Bansal, et al. MathVista: Evaluating mathematical reasoning of foundation models in visual contexts. *arXiv preprint arXiv:2310.02255*, 2023. ICLR 2024. 8

[26] Hamed Mahdavi, Pouria Mahdavinia, Alireza Farhadi, Pegah Mohammadipour, Samira Malek, Pedram Mohammadipour, Majid Daliri, Alireza Hashemi, Amir Khasahmadi, and Vasant G. Honavar. Combigraph-vis: A curated multimodal olympiad benchmark for discrete mathematical reasoning. *arXiv preprint arXiv:2510.27094*, 2025. 3

[27] ModelScope Community. Evalscope: A streamlined and customizable framework for model evaluation. <https://github.com/modelscope/evalscope>, 2025. Documentation: <https://evalscope.readthedocs.io/>. 3

[28] NVIDIA. Nemo evaluator sdk — code generation containers (default parameters). <https://docs.nvidia.com/nemo/evaluator/latest/libraries/nemo-evaluator/containers/code-generation.html>, 2025. Lists default max_new_tokens=2048. 3

[29] Qwen Team. Qwen3-vl. <https://github.com/QwenLM/Qwen3-VL>, 2025. Release notes and model cards (Oct 4/15/21, 2025). 2

[30] Daniel Rose et al. Visual chain of thought: Bridging logical gaps with multimodal infillings. *arXiv preprint arXiv:2305.02317*, 2023. 2

[31] Sreetama Sarkar, Yue Che, Alex Gavin, Peter A. Beerel, and Souvik Kundu. Mitigating hallucinations in vision-language models through image-guided head suppression. *arXiv preprint arXiv:2505.16411*, 2025. 3

[32] Hossam Sheta, Omkar Sardesai, Josep Crego, Xiang Ren, Eunsol Choi, David Alvarez-Melis, Alexandra DeLucia, Yang Zhang, and Ebrahim Bagheri. Interpreting vision-language models with vlm-lens. In *Proceedings of the 2025 Conference on Empirical Methods in Natural Language Processing: System Demonstrations*, 2025. 3

[33] Weikang Shi et al. Mathcanvas: Intrinsic visual chain-of-thought for multimodal mathematical reasoning. *arXiv preprint arXiv:2510.14958*, 2025. 2

[34] Renliang Sun, Wei Cheng, Dawei Li, Haifeng Chen, and Wei Wang. Stop when enough: Adaptive early-stopping for chain-of-thought reasoning. *arXiv preprint arXiv:2510.10103*, 2025. 2, 6, 7

[35] Yunlong Tang, Jing Bi, Chao Huang, Susan Liang, Daiki Shimada, Hang Hua, Yunzhong Xiao, Yizhi Song, Pinxin Liu, Mingqian Feng, Junjia Guo, Zhuo Liu, Luchuan Song, Ali Vosoughi, Jinxi He, Liu He, Zeliang Zhang, Jiebo Luo, and Chenliang Xu. Caption anything in video: Fine-grained object-centric captioning via spatiotemporal multimodal prompting, 2025. 2

[36] Yolo Yunlong Tang, Jing Bi, Pinxin Liu, Zhenyu Pan, Zhangyun Tan, Qianxiang Shen, Jiani Liu, Hang Hua, Junjia Guo, Yunzhong Xiao, Chao Huang, Zhiyuan Wang, Susan Liang, Xinyi Liu, Yizhi Song, Junhua Huang, Jia-Xing Zhong, Bozheng Li, Daiqing Qi, Ziyun Zeng, Ali Vosoughi, Luchuan Song, Zeliang Zhang, Daiki Shimada, Han Liu, Jiebo Luo, and Chenliang Xu. Video-lmm post-training: A deep dive into video reasoning with large multimodal models, 2025. 3

[37] Sree Harsha Tanneru et al. On the hardness of faithful chain-of-thought reasoning in large language models. *arXiv preprint arXiv:2406.10625*, 2024. 1

[38] Vals.ai. Mmmu benchmark (evaluation settings and runs). <https://www.vals.ai/benchmarks/mmmu>, 2025. Accessed: 2025-11-11. 3

[39] Kai Wang, Ruili Zhang, et al. Measuring multimodal mathematical reasoning with the MATH-Vision dataset. *arXiv preprint arXiv:2402.14804*, 2024. NeurIPS 2024. 8

[40] Peng Wang et al. Qwen2-vl: Enhancing vision-language model's capabilities with naive dynamic resolution. *arXiv preprint arXiv:2409.12191*, 2024. 2

[41] Weiyun Wang, Zhangwei Gao, Lixin Gu, Hengjun Pu, Long Cui, Xinguang Wei, Zhaoyang Liu, Linglin Jing, Shenglong Ye, Jie Shao, Zhaokai Wang, Zhe Chen, Hongjie Zhang, Ganlin Yang, Haomin Wang, Qi Wei, Jinhui Yin, Wenhao Li, Erfei Cui, Guanzhou Chen, Zichen Ding, Changyao Tian, Zhenyu Wu, Jingjing Xie, Zehao Li, Bowen Yang, Yuchen Duan, Xuehui Wang, Songze Li, Xiangyu Zhao, Haodong Duan, Nianchen Deng, Bin Fu, Yinan He, Yi Wang, Conghui He, Botian Shi, Junjun He, Yingtong Xiong, Han Lv, Lijun Wu, Wenqi Shao, Kaipeng Zhang, Huipeng Deng, Biqing Qi, Jiaye Ge, Qipeng Guo, Wenwei Zhang, Wanli Ouyang, Limin Wang, Min Dou, Xizhou Zhu, Tong Lu, Dahua Lin, Jifeng Dai, Bowen Zhou, Weijie Su, Kai Chen, Yu Qiao, Wenhui Wang, and Gen Luo. Internvl3.5: Advancing open-source multimodal models in versatility, reasoning, and efficiency. *arXiv preprint arXiv:2508.18265*, 2025. 2

[42] Weiyun Wang, Zhangwei Gao, Lixin Gu, Hengjun Pu, Long Cui, Xinguang Wei, Zhaoyang Liu, Linglin Jing, Shenglong Ye, Jie Shao, et al. Internvl3.5: Advancing open-source multimodal models in versatility, reasoning, and efficiency. *arXiv preprint arXiv:2508.18265*, 2025. 3

[43] Wei Wang et al. Internvl 3.5: Advancing open-source multimodal models with versatile capabilities. *arXiv preprint arXiv:2508.18265*, 2025. 2

[44] Xuezhi Wang, Jason Wei, Dale Schuurmans, Quoc Le, Ed Chi, Sharan Narang, Aakanksha Chowdhery, and Denny Zhou. Self-consistency improves chain of thought reasoning in language models. *arXiv preprint arXiv:2203.11171*, 2022. 3

[45] Qiong Wu et al. Grounded chain-of-thought for multimodal large language models. *arXiv preprint arXiv:2503.12799*, 2025. 1, 2

[46] Guowei Xu, Peng Jin, Hao Li, Yibing Song, Lichao Sun, and Li Yuan. Llava-cot: Let vision language models reason step-by-step. *arXiv preprint arXiv:2411.10440*, 2024. 2

[47] Tianyang Xu et al. Dynamic early exit in reasoning models. *arXiv preprint arXiv:2504.15895*, 2025. 2

[48] Chenxu Yang, Qingyi Si, Yongjie Duan, Zheliang Zhu, Chenyu Zhu, Zheng Lin, Li Cao, and Weiping Wang. Dynamic early exit in reasoning models. *arXiv preprint arXiv:2504.15895*, 2025. 7

[49] Huanjin Yao, Jiaxing Huang, Wenhao Wu, Jingyi Zhang, Yibo Wang, Shunyu Liu, Yingjie Wang, Yuxin Song,

Haocheng Feng, Li Shen, and Dacheng Tao. Mulberry: Empowering mllm with o1-like reasoning and reflection via collective monte carlo tree search. *arXiv preprint arXiv:2412.18319*, 2024. 2

[50] Enoch Yeo et al. Demystifying long chain-of-thought reasoning in llms. *arXiv preprint arXiv:2502.03373*, 2025. 1

[51] Xiang Yue, Yuansheng Ni, Kai Zhang, Tianyu Zheng, Ruoqi Liu, Ge Zhang, Samuel Stevens, Dongfu Jiang, Weiming Ren, Yuxuan Sun, et al. Mmmu: A massive multi-discipline multimodal understanding and reasoning benchmark for expert agi. In *Proceedings of the IEEE/CVF Conference on Computer Vision and Pattern Recognition (CVPR)*, 2024. 3

[52] Kaichen Zhang, Bo Li, Peiyuan Zhang, Fanyi Pu, Joshua Adrian Cahyono, Kairui Hu, Shuai Liu, Yuanhan Zhang, Jingkang Yang, Chunyuan Li, and Ziwei Liu. Lmms-eval: Reality check on the evaluation of large multimodal models. *arXiv preprint arXiv:2407.12772*, 2024. 3

[53] Kaichen Zhang et al. Lmms-eval: Reality check on the evaluation of large multimodal models. *arXiv preprint arXiv:2407.12772*, 2024. 1

[54] Ruili Zhang, Kai Wang, et al. MathVerse: Does your multi-modal LLM truly see the diagrams? *arXiv preprint arXiv:2403.14624*, 2024. ECCV 2024. 8

[55] Yuanhan Zhang et al. Evaluating and steering modality preferences in multimodal large language model. *arXiv preprint arXiv:2505.20977*, 2025. 1

[56] Chengshuai Zhao, Zhen Tan, Pingchuan Ma, Dawei Li, Bohan Jiang, Yancheng Wang, Yingzhen Yang, and Huan Liu. Is chain-of-thought reasoning of llms a mirage? a data distribution lens. *arXiv preprint arXiv:2508.01191*, 2025. 2

[57] Haojie Zheng et al. Thinking before looking: Improving multimodal llm reasoning via mitigating visual hallucination. *arXiv preprint arXiv:2411.12591*, 2024. 1, 2

[58] Y. Zhou et al. Mira: A benchmark for visual chain-of-thought. *arXiv preprint arXiv:2511.02779*, 2025. 3

[59] Jiaqi Zhu et al. Internvl3: Exploring advanced training and test-time scaling for multimodal foundation models. *arXiv preprint arXiv:2504.10479*, 2025. 2